

# Quantum Spin Hall Effect and Diamagnetism in Bismuth

Shuichi Murakami\*

Department of Applied Physics, University of Tokyo, Hongo, Bunkyo-ku, Tokyo 113-8656, Japan

We show that the spin Hall conductivity in insulators is related with a magnetic susceptibility representing the strength of the spin-orbit coupling. We use this relationship as a guiding principle to search real materials showing quantum spin Hall effect. As a result, we demonstrate that bismuth will show the quantum spin Hall effect, both by calculating the helical edge states, and by showing the non-triviality of the  $Z_2$  topological number, and propose possible experiments.

PACS numbers: 73.43.-f, 72.25.Dc, 72.25.Hg, 85.75.-d

Spin Hall effect (SHE) [1, 2, 3] has been attracting much attention recently, partly due to potential use for semiconductor spintronics. A remarkable feature is that a spin current can be induced without breaking time-reversal symmetry. One of the interesting proposals is the quantum spin Hall (QSH) phase in [4, 5, 6, 7, 8, 9], which is a 2D insulator with “helical” edge states. The edge states form Kramers pairs, with spin current flowing in the opposite way for the two spin directions. For its scientific interest akin to the quantum Hall systems, an experimental observation of the QSH phase is called for.

To analyze robustness of edge states,  $Z_2$  topological number is proposed [6]. This corresponds to a number of pairs of helical edge states modulo two, and odd or even topological number corresponds to the QSH and spin-Hall-insulator (SHI) [10] phases, respectively. The SHI is topologically equivalent to a simple insulator, and is commonly found [10]. To search for candidate materials for the QSH phase among a vast number of nonmagnetic insulators, we need a guiding principle. We propose that the magnetic susceptibility would be a good measure for searching candidate materials. From this viewpoint, in this paper we pick up bismuth as a candidate for the QSH phase due to its large diamagnetic susceptibility. There are also other supporting clues: large spin splitting in the surface states of the 3D system, suggesting similar edge states for the 2D systems, the crystal structure in the (111) plane similar the Kane-Mele model for the QSH phase [6]. Using a 2D tight-binding model which reflects the real band structure, we show that this system has only one pair of edge modes. We also show that its  $Z_2$  topological number [6] is odd, i.e. nontrivial, which supports stability of the edge state. These aspects makes bismuth a promising candidate for the QSH phase.

To relate the magnetic susceptibility with the spin Hall conductivity (SHC), we derive here a spin-Hall analog of the Středa formula. The Středa formula [11, 12] tells us that in insulators the Hall conductivity  $\sigma_{xy}$  is expressed as  $\sigma_{xy} = \frac{e}{\Omega} \frac{\partial N}{\partial B} |_{\mu}$ , where  $N$  is the number of states below the chemical potential  $\mu$ , and  $\Omega$  is the area of the system. A straightforward generalization to the spin problem is to replace  $N$  by the spin  $s_z$ , i.e.  $\sigma_s = \frac{1}{\Omega} \frac{\partial s_z}{\partial B} |_{\mu}$ . This is physically reasonable from the following argument. Sup-

pose we apply a magnetic field in some region, linearly increasing in time. Then a change of the total spin inside the region will be proportional to  $\frac{\partial s_z}{\partial B} |_{\mu}$ . According to the Maxwell equation, the increasing magnetic field induces a circulating electric field. Therefore, by interpreting the spin change as due to a spin Hall current by the electric field, the SHC is  $\sigma_s = \frac{1}{\Omega} \frac{\partial s_z}{\partial B} |_{\mu}$ . This physical picture is justified by the following calculations.

A key step is to use a “conserved” spin current [13]. In most papers on the SHC, the spin current is defined as a symmetrized product of spin and velocity:  $\vec{J}_s = \frac{1}{2} \{ \vec{v}, s_z \}$ . However, in the presence of the spin-orbit coupling, the spin is no longer conserved:  $\mathcal{T} \equiv \dot{s}_z \neq 0$ . Namely, the rhs of the equation of continuity,  $\partial_t s_z + \vec{\nabla} \cdot \vec{J}_s = \mathcal{T}$  is nonzero, and the “conventional” spin current  $\vec{J}_s$  is not directly related with spin accumulation. Instead, Shi *et al.* [13] defined a conserved spin current  $\vec{J}_s$  as follows. If the system satisfies  $\int dV \mathcal{T} = 0$ , as it does in a uniform electric field, the torque term  $\mathcal{T}$  can be written as  $-\vec{\nabla} \cdot \vec{P}_{\tau}$ . Thus we get  $\partial_t s_z + \vec{\nabla} \cdot \vec{J}_s = 0$ , where  $\vec{J}_s \equiv \vec{J}_s + \vec{P}_{\tau}$  is called a conserved spin current. The SHC for the conserved spin current is calculated for several models [13, 14].

To calculate the SHC for the conserved spin current, we consider an electric field with wavenumber  $q$ , and take the limit  $q \rightarrow 0$  [13]. When we calculate a spin current flowing to the  $x$ -direction in response to an electric field to the  $y$ -direction, we take the vector potential  $\vec{A} = A_y e^{iqx} \hat{y}$ , and the response is calculated as

$$\sigma_s^{\mathcal{J}} = -\frac{e}{\Omega} \lim_{q \rightarrow 0} i \partial_q \sum_{n \neq m} \frac{f(\varepsilon_m) - f(\varepsilon_n)}{(\varepsilon_n - \varepsilon_m)(\varepsilon_n - \varepsilon_m + i\eta)} \langle n | [H, s_z e^{iqx}] | m \rangle \langle m | \frac{1}{2} \{ v_y, e^{-iqx} \} | n \rangle. \quad (1)$$

By a calculation similar to [15], it can be simplified as

$$\begin{aligned} \sigma_s^{\mathcal{J}} &= \sigma_s^{\mathcal{J}(I)} + \sigma_s^{\mathcal{J}(II)}, \\ \sigma_s^{\mathcal{J}(I)} &= \frac{ie}{8\pi\Omega} \int d\varepsilon \frac{df}{d\varepsilon} \text{tr} \left( ([H, s_z] G_+ \{ v_y, x \} \right. \\ &\quad \left. - \{ v_y, x \} G_- [H, s_z] - 2[H, s_z x] G_+ v_y \right. \\ &\quad \left. + 2v_y G_- [H, s_z x] + [x, [s_z, v_y]] \right) (G_+ - G_-), \\ \sigma_s^{\mathcal{J}(II)} &= \frac{ie}{\Omega} \int \frac{d\varepsilon}{4\pi} f(\varepsilon) \text{tr} (s_z G_+ L_z G_+ - G_- L_z G_-) \end{aligned} \quad (2)$$

where  $G_{\pm} = (\varepsilon - H \pm i\eta)^{-1}$  and  $L_z = xv_y - yv_x$  is an orbital angular momentum. The term  $\sigma_s^{\mathcal{J}(I)}$  is proportional to  $\frac{d\varepsilon}{d\varepsilon}(G_+ - G_-)$ . By noting  $G_+ - G_- = -2\pi i\delta(\varepsilon - H)$ , only the states at the Fermi energy contribute to  $\sigma_s^{\mathcal{J}(I)}$ . In insulators  $\sigma_s^{\mathcal{J}(I)}$  vanishes identically. On the other hand, the second term  $\sigma_s^{\mathcal{J}(II)}$  is expressed as

$$\sigma_s^{\mathcal{J}(II)} = \int \frac{d\varepsilon}{\Omega} f(\varepsilon) \text{tr} \left( s_z \frac{d\delta(\varepsilon - H)}{dB_{\text{orb}}} \right) = \frac{1}{\Omega} \frac{ds_z}{dB_{\text{orb}}}. \quad (3)$$

Equation (3) agrees with the physically expected form. This result (3) can be also written as

$$\sigma_s^{\mathcal{J}(II)} = \frac{-\hbar}{g\mu_B} \frac{1}{\Omega} \frac{dM_{\text{orb.}}}{dB_{\text{Zeeman}}} = \frac{1}{\Omega g} \frac{dL_z}{dB_{\text{Zeeman}}}. \quad (4)$$

where  $g$  is the electron-spin  $g$ -factor,  $M_{\text{orb.}}$  is an orbital magnetization, and  $\mu_B$  is the Bohr magneton. These formulae are a spin analog of the Středa formula [12]. We note that a Středa formula for the SHC with the conventional spin current  $\vec{J}_s$  [15] has extra terms involving  $\dot{s}_z$ , in addition to (3). These terms arise from spin nonconservation. Hence it is natural that they do not appear in (3), as we used the conserved spin current. We remark that the definition of the spin current is still a controversial issue. Since the spin is not conserved, there is no unique definition of the spin current. Because there is no established way of directly measuring the spin current itself, one way is to consider instead a measurable quantities such as spin accumulation at edges. The spin accumulation depends crucially on boundary conditions, and the conserved spin current may correspond to smooth boundaries [13]. This point requires further investigation.

We calculate  $\sigma_s$  for the model on the honeycomb lattice proposed by Kane and Mele [6]. This model shows the SHI and the QSH phases, depending on parameters  $\lambda_R$ ,  $\lambda_v$  and  $\lambda_{SO}$ . We numerically evaluate the SHC by Eq. (4) using the formula of orbital magnetization [16, 17],

$$M_{\text{orb.}} = \frac{ei}{2\hbar} \sum'_n \int \frac{d^d k}{(2\pi)^d} \left\langle \frac{\partial u_{n\mathbf{k}}}{\partial \mathbf{k}} \right| \times (2\mu - \varepsilon_{n\mathbf{k}} - H) \left| \frac{\partial u_{n\mathbf{k}}}{\partial \mathbf{k}} \right\rangle, \quad (5)$$

where  $\sum'_n$  is a sum over occupied bands. The result is shown in Fig. 1. The calculated SHC is  $\sigma_s \sim 0$  in the SHI phase and  $\sigma_s \sim -\frac{e}{(2\pi)}$  in the QSH phase, except for the vicinity of the phase boundary. The SHC in the QSH phase,  $\sigma_s \sim -e/(2\pi)$ , is interpreted as a fundamental unit  $e/(4\pi)$  times two, the number of the edge states. The quantization is exact when  $s_z$  is a good quantum number, i.e.  $\lambda_R = 0$ , where the system is a superposition of two quantum Hall systems with  $\sigma_{xy} = \pm e^2/h$ . Remarkably, even when  $s_z$  is no longer conserved, the SHC remains almost quantized. Deviation from the quantized value is more prominent near the phase boundaries, which is attributed to smallness of the band gap.

Therefore, materials with large susceptibility would be a good candidate for the QSH phase. Namely, if the sus-

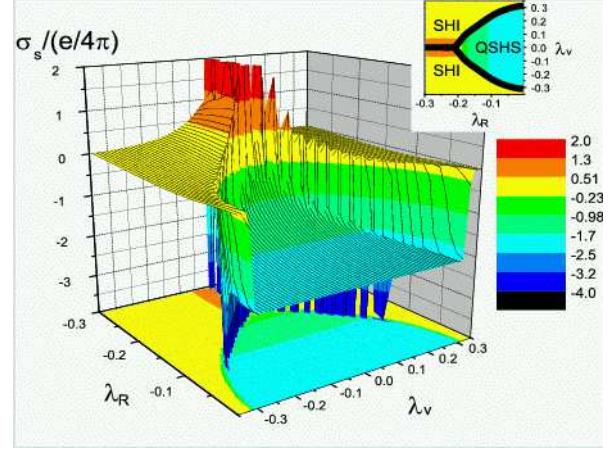


FIG. 1: Spin Hall conductivity  $\sigma_s$  for the Kane-Mele model on the honeycomb lattice for various values of  $\lambda_R$  and  $\lambda_v$  in the unit of  $t$ .  $\lambda_{SO}$  is fixed as  $0.06t$ . As it is symmetric with respect to  $\lambda_R \rightarrow -\lambda_R$ , we show only the result for negative  $\lambda_R$ . The phase diagram is shown in the inset. Except for the vicinity of the phase boundary,  $\sigma_s \sim 0$  in the SHI phase, and  $\sigma_s \sim -e/(2\pi)$  in the QSH phase.

ceptibility is large,  $\sigma_s$  should be large. Figure 1 then suggests that the system should be either in the QSH phase or near the phase boundary to the QSH phase. From this reason, we pick up some semimetals and related materials with large diamagnetic susceptibility, among which are bismuth and graphite.

Bi crystal has a rhombohedral structure, with trigonal symmetry around the (111) axis. Bi is a semimetal with a small hole pocket at the  $T$  point, and three electron pockets at the  $L$  points. Its large diamagnetic susceptibility have been studied both experimentally and theoretically. It is theoretically attributed to massive Dirac fermions at the  $L$  and  $T$  points [18]. These Dirac fermions gives a diamagnetic susceptibility which is enhanced as logarithm of the (small) energy gap [18]. This picture is valid, even when the Fermi energy is in the gap, and the susceptibility is larger when the Fermi energy is in the gap. Such Dirac fermions contribute to anomalous Hall effect and the SHE. Hence, it is no wonder such enhanced diamagnetic susceptibility implies an enhanced charge/spin Hall conductivity.

Because the QSH phase is in 2D, we have to make Bi two-dimensional, such as thin films and quantum wells. Such confinement discretizes the perpendicular momentum, and tends to open the gap. It was theoretically proposed that by making the Bi film thinner, it turns from semimetal to semiconductor [19, 20]. Experiments show that the gap may open in thinner samples, whereas the gap is obscured by carrier unbalance between holes and electrons [21]. Remarkably, the lattice structure of Bi in the (111) plane resembles the Kane-Mele model [6]. The crystal can be viewed as a stacking of bilayers along the [111] direction. The inter-bilayer coupling is much

smaller than the intra-bilayer one, and the LEED analysis showed that the (111) surface of Bi is terminated with an intact bilayer [22]. Crystal structure of a single bilayer (Fig. 2(a)) consists of two triangular sublattices located in different layers. This honeycomb-like lattice structure is a key for a nontrivial  $Z_2$  topological number; a crystal structure with high symmetry (e.g. square lattice) favors a trivial  $Z_2$  topological number.

We now demonstrate that 2D single-bilayer bismuth possesses a pair of helical edge states carrying spin currents with opposite spins. Furthermore, we show that the  $Z_2$  topological number is odd. For these purposes, we use the 3D tight-binding model [23] which well reproduces the band structure, and truncate the model by retaining only the hoppings inside the bilayer. The resulting 16-band model is regarded as a multi-orbital version of the Kane-Mele model. We first calculate the band structure for a single bilayer (Fig. 2(a)) for a strip geometry. The result is shown in Fig. 2(b), where projected bulk bands are shown in gray. The figure shows four edge states connecting between the bulk conduction and valence bands. They correspond to one Kramers pair of edge states (at the two edges), suggesting nontrivial (odd)  $Z_2$  topological invariant. To confirm this, we also calculate the Pfaffian  $\text{Pf}(\mathbf{k})$  to calculate the  $Z_2$  topological number [6]. The bilayer system is inversion-symmetric, allowing  $\text{Pf}(\mathbf{k})$  to be chosen real. The result is Fig. 2(c), where  $\text{Pf}(\mathbf{k})$  changes sign at the red curve, corresponding to Fig. 2 (a) in [6]; it implies odd  $Z_2$  number. To further clarify the phase winding of  $\text{Pf}(\mathbf{k})$ , we break the inversion symmetry by adding small on-site energies  $\pm v$ , for the atoms on the upper and the lower layers, respectively. This may correspond to a heterostructure or a single-bilayer thin film on a substrate. The result is shown in Fig. 2(d) for  $v = 0.2\text{eV}$ . There is only one vortex for the phase of  $\text{Pf}(\mathbf{k})$  in the half BZ, which ensures the odd  $Z_2$  number, corresponding to Fig. 2(b) in [6]. We note that the zeros of the Pfaffian do not follow the threefold rotational symmetry. It is because the Pfaffian is not covariant with respect to unitary transformation of the Hamiltonian, and depends on a choice of the unit cell. Because this QSH phase is protected by topology, it cannot be broken unless the valence and conduction bands touch at the same wavenumber and the direct gap closes. Therefore, even though the 2D tight-binding model might not reproduce quantitatively the real band structure, the nontriviality of the  $Z_2$  index is more robust. This nontrivial  $Z_2$  number guarantees stability of the helical edge states [7, 8]. Only when the  $Z_2$  topological number is odd, the edge states are stable against single-particle backscattering and (reasonably weak) two-particle backscattering, whereas for even topological number, the edge state will be gapped in general [7, 8]. For example, in a bilayer antimony, we found that there are two pairs of edge modes, and the  $Z_2$  number is even. Thus the edge modes in 2D antimony will be fragile against opening a gap.

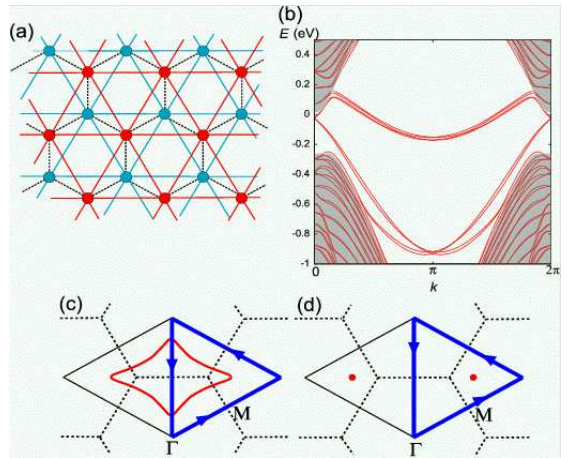


FIG. 2: Calculation on the bilayer tight-binding model of bismuth in the (111) plane. The crystal structure of the (111)-bilayer bismuth is shown in (a), where the upper and lower layers are denoted by red and blue, respectively. The solid and broken lines denote intralayer and interlayer hoppings, respectively. (b) is the calculated band structure for the strip geometry. The gray region is the bulk bands, while the red curves are the states calculated for a strip with width of 20 lattice sites. Zeros of the Pfaffian  $\text{Pf}(\mathbf{k})$  in the Brillouin zone are shown in red for (c) the inversion-symmetric case ( $v = 0$ ) and for (d) the inversion-asymmetric case ( $v = 0.2\text{eV}$ ).

We now discuss a multilayer Bi thin film. Bismuth is suitable for pursuit of quantum size effects. A long mean-free path ( $l \sim \mu\text{m-mm}$ ) [24], large electron mobility up to  $10^6\text{cm}^2/\text{Vs}$  at 5K [25], and a small effective mass of electrons make the semimetal bismuth a good material to see quantum-size effects even at room temperature [26]. Furthermore, Bi thin films can be synthesized with good quality. For example, a  $10\ \mu\text{m}$ -thick film shows magnetoresistance with a factor of few thousands at 5K and a factor of 2-3 at room temperature [25, 27].

By stacking  $N$  bilayers, the direct gap never closes, and each edge mode is topologically protected; the number of pairs of edge modes becomes  $N$ . When the film becomes thicker, the helical edge states are expected to evolve to 2D surface states on a 3D bulk Bi, which has been studied by the angle-resolved photoemission spectroscopy [28, 29, 30]. The surface states with large spin splitting is observed [30], which manifests spin currents carried by such surface states. If the film thickness  $D$  is less than the mean free path  $l$ , e.g.  $D \sim 10\ \mu\text{m}$  [25, 27], each of these edge modes has a quantized motion in the perpendicular direction. Hence, although the backscattering is relevant for even  $N$ , its effect on the edge states is almost negligible, and the system becomes gapless. By lowering the temperature or by increasing the disorder, the system will eventually become the SHI or the QSH phases depending on whether  $N$  is even or odd.

To observe the QSH phase experimentally, one way is to measure the spin current by an applied electric field.

However, the QSH phase does not show a quantization [6], and it may be elusive to establish the QSH phase, compared with the quantum Hall effect (QHE). On the other hand, the critical exponent  $\nu$ , governing the localization length is different between the QSH and the SHI phases [31]. Thus, the QSH phase can be established via measurement of  $\nu$ . In the QHE,  $\nu$  is determined experimentally by changing the magnetic field across the plateau transition [32, 33, 34], because the change of the magnetic field controls the Fermi energy across the extended state. In the QSH phase, for example by a change of a gate voltage, one may be able to control the Fermi energy to the extended or localized states. To determine  $\nu$ , one has to see the range of the gate voltage  $\Delta V_g$  showing nonzero  $\sigma_{xx}$  by varying the sample size [34] or the temperature [33]. From their critical exponents,  $\nu$  is calculated.

Another way to establish the QSH phase is to observe the edge states by scanning tunneling microscopy/spectroscopy, as has been used for graphite [35, 36]. There is one important difference between the edge states of the graphite and the QSH phase. In graphene the existence of edge states crucially depends on the edge shape; the zigzag edge has edge states while the armchair edge does not. For a rough edge with portions of zigzag and armchair edges, only at the zigzag edges can the signal of edge states be seen [36]. In contrast, the edge states in the QSH phase carry helical spin currents, and circulate along the whole edge around, irrespective of the details (e.g. the shape) of the edge.

Besides bismuth, graphite is another material with anomalously large diamagnetic susceptibility [37]. The spin-orbit coupling of graphite is small, and the diamagnetism is mostly carried by orbital motion. In the same token as the SHE, the orbital-angular-momentum (OAM) Hall effect can be studied [38]. The resulting OAM Hall conductivity is the susceptibility for the orbital:  $\sigma_{\text{OAM}}^{\mathcal{J}(II)} = \frac{1}{\Omega} \frac{dL_z}{dB_{\text{orb}}}$ . Since this involves only the orbital, the spin-orbit coupling is not required for it to be nonzero. Because the orbital susceptibility is largely enhanced in the graphite due to massless Dirac fermions, graphite will show large OAM current,

In conclusion, we show that the SHC is directly related with the magnetic susceptibility, and we propose this as a criterion for search of quantum spin Hall systems. We show that 2D bismuth will show the quantum spin Hall effect, because the number of pairs of helical edge states is odd and the  $Z_2$  topological number is nontrivial. The surface states with large spin splitting in bulk bismuth, might be closely related with these edge modes.

We thank B. A. Bernevig, M.-C. Chang, N. Nagaosa, and S.-C. Zhang for helpful discussions. This research was supported in part by Grant-in-Aid from the Ministry of Education, Culture, Sports, Science and Technology of Japan and by the National Science Foundation under Grant No. PHY99-07949.

\* Electronic address: murakami@appi.t.u-tokyo.ac.jp

---

- [1] M. I. D'yakonov and V. I. Perel', Phys. Lett. A **35**, 459 (1971).
- [2] S. Murakami, N. Nagaosa, and S.-C. Zhang, Science **301**, 1348 (2003).
- [3] J. Sinova *et al.*, Phys. Rev. Lett. **92**, 126603 (2004).
- [4] B. A. Bernevig and S.-C. Zhang, Phys. Rev. Lett. **96**, 106802 (2006).
- [5] X.-L. Qi, Y.-S. Wu and S.-C. Zhang, cond-mat/0505308.
- [6] C. L. Kane and E. J. Mele, **95**, 146802 (2005); *ibid.* **95**, 226801 (2005).
- [7] C. Wu, B. A. Bernevig, and S.-C. Zhang, Phys. Rev. Lett. **96**, 106401 (2006).
- [8] C. Xu and J. E. Moore, Phys. Rev. B **73**, 045322 (2006).
- [9] M. Onoda and N. Nagaosa, Phys. Rev. Lett. **95**, 106601 (2005).
- [10] S. Murakami, N. Nagaosa, and S.-C. Zhang, Phys. Rev. Lett. **93**, 156804 (2004)
- [11] L. Smrčka and P. Středa, J. Phys. C: Solid State Phys. **10**, 2153 (1977).
- [12] P. Středa, J. Phys. C: Solid State Phys. **15**, L717 (1982).
- [13] J. Shi *et al.*, Phys. Rev. Lett. **96**, 076604 (2006).
- [14] N. Sugimoto *et al.*, Phys. Rev. B **73**, 113305 (2006).
- [15] M.-F. Yang and M.-C. Chang, Phys. Rev. B **73**, 073304 (2006).
- [16] D. Xiao, J. Shi, and Q. Niu, Phys. Rev. Lett. **95**, 137204 (2005).
- [17] T. Thonhauser *et al.*, Phys. Rev. Lett. **95**, 137205 (2005).
- [18] H. Fukuyama and R. Kubo, J. Phys. Soc. Jpn. **28**, 570 (1970); F. A. Buot and J. W. McClure, Phys. Rev. B **6**, 4525 (1972).
- [19] V. N. Lutskii, Pis'ma Zh. Eksp. Teor. Fiz. **2**, 391 (1965) [JETP Lett. **2**, 245 (1965)].
- [20] V. B. Sandomirskii, Zh. Eksp. Teor. Fiz. **52**, 158 (1967) [Sov. Phys. JETP **25**, 101 (1967)].
- [21] C. A. Hoffman *et al.*, Phys. Rev. B **48**, 11431 (1993); H. T. Chu, Phys. Rev. B **51**, 5532 (1995); C. A. Hoffman *et al.*, *ibid.* **51**, 5535 (1995); M. Lu *et al.*, Phys. Rev. B **53**, 1609 (1996).
- [22] H. Mönig *et al.*, Phys. Rev. B **72**, 085410 (2005).
- [23] Y. Liu and R. E. Allen, Phys. Rev. B **52**, 1566 (1995).
- [24] D. H. Reneker, Phys. Rev. Lett. **1**, 440 (1958); W. S. Boyle and G. E. Smith, Prog. Semicond. **7**, 1 (1963).
- [25] S. Cho *et al.*, Appl. Phys. Lett. **79**, 3651 (2001).
- [26] E. I. Rogacheva *et al.*, Appl. Phys. Lett. **82**, 2628 (2003).
- [27] F. Y. Yang *et al.*, Science **284**, 1335 (1999).
- [28] C. R. Ast and H. Höchst, Phys. Rev. Lett. **90**, 016403 (2003); Phys. Rev. B **67**, 113102 (2003).
- [29] T. K. Kim *et al.*, Phys. Rev. B **72**, 085440 (2005).
- [30] Yu. M. Koroteev *et al.*, Phys. Rev. Lett. **93**, 046403 (2004).
- [31] M. Onoda, Y. Avishai, N. Nagaosa, cond-mat/0605510.
- [32] B. Huckestein, Rev. Mod. Phys. **67**, 357 (1995).
- [33] H. P. Wei *et al.*, Phys. Rev. Lett. **61**, 1294 (1988).
- [34] S. Koch *et al.*, Phys. Rev. Lett. **67**, 883 (1991).
- [35] Y. Niimi *et al.*, Phys. Rev. B **73**, 085421 (2006).
- [36] Y. Kobayashi *et al.*, Phys. Rev. B **71** (2005) 193406.
- [37] J. W. McClure, Phys. Rev. **104**, 666 (1956); *ibid.* **119**, 606 (1960).
- [38] S. Zhang and Z. Yang, Phys. Rev. Lett. **94**, 066602 (2005).